Journal of Sustainable Mining 16 (2017) 94–103

HOSTED BY

Contents lists available at ScienceDirect

Journal of Sustainable Mining

journal homepage: http://www.elsevier.com/locate/jsm

Research paper

Geomechanical analysis of location and conditions for mining-induced tremors in LGOM copper mines

Jerzy Cieślik*, Zbigniew Burtan, Dariusz Chlebowski, Andrzej Zorychta

AGH University of Science and Technology, Poland

ARTICLE INFO

Article history:
Received 6 July 2017
Received in revised form
29 September 2017
Accepted 12 October 2017
Available online 15 October 2017

Keywords:
Mining geomechanics
Seismic hazard
FEM calculations

ABSTRACT

This paper presents the results of the statistical analyses of rock mass seismicity associated with O/ZG Rudna exploitation and geomechanical analyses concerning the location and conditions of tremor occurrences in LGOM conditions, illustrated by the example of O/ZG Rudna.

As part of the statistical analyses, the assessment of rock mass seismicity formation in O/ZG Rudna throughout the whole mine area in the years 2006–2015 is presented, the results of which were the basis for subsequent geo-mechanical analyses. Within the parameters of seismic activity, the analysis covered the number of recorded events, the total value of energy emission and the index of individual energy expenditure. The presented analyses also refer to the locations of tremor source epicentres in relation to the exploitation front, distinguished into low energy and high energy tremors located ahead of the exploitation front, in the area of opening-up works and gobs. These recent results were the starting point for research and calculations on geo-mechanical analyses. These numerical calculations using the finite element method (FEM) carried out the energy density distribution of elastic deformation in the vicinity of the exploitation front. FEM calculations were designed to establish the factors and conditions that determine the location of tremor sources and the mechanism of rock destruction. Both of these factors are directly related to the magnitude of the energy emitted during the tremor. Appropriate energy measurements of elastic deformation have been adopted to determine rock mass areas which are potentially threatened by tremor occurrences of varying energy. Measures of the energy density of shear and volumetric strain enable the determination of the nature of rock mass destruction in the vicinity of mine workings, which in turn gives the basis for linking these measurements with tremor energy and location relative to the exploitation front. The results of numerical computations were compared with the results of statistical analyses on the locations of tremor sources with different energies in relation to the exploitation front in O/ZG Rudna.

1. Introduction

The current high level of rockburst hazards in LGOM mines is a consequence of rock mass seismicity accompanying mining operation, and the majority of the rockbursts and distressing events recorded so far have been caused by high-energy tremors. High-energy tremors, which have a huge influence on the magnitude of rockburst occurrence, are a natural feature of copper ore deposits in LGOM, resulting from the occurrence of tremor-prone rock formations above the exploited deposit (Chlebowski, 2011; Kłeczek, 2006, 2007), as well as periodic activation of faulting (Burtan, 2011). The analysis of seismic activity recorded in recent years in LGOM areas shows that the most seismically active mine is O/ZG Rudna. This is the result of both natural conditions, which are expressed primarily by the high depth of exploitation, the aforementioned thick-layered rock mass structure and the occurrence of tectonic disturbances, but also the need to extract fields in areas with significant exploitation involvement, i.e. exploitation of the deposit residue or in the vicinity of gobs. The seismic activity of rock mass is also influenced by active rockburst prevention (Kłeczek, 2007; Zorychta, Burtan, & Chlebowski, 2005). This paper presents the formation of rock mass seismicity in O/ZG Rudna from 2006 to 2015 in the whole mine area. Seismic activity of the rock mass was characterized by the number of recorded events, the total value of energy emission and the index of the individual energy

* Corresponding author. AGH University of Science and Technology, al. Mickiewicza 30, 30-059 Krakow, Poland.
E-mail address: jerzy.cieslik@agh.edu.pl (J. Cieślik).

https://doi.org/10.1016/j.jsm.2017.10.002

expenditure. The results of these analyses, performed for the O/ZG Rudna area, were the basis for investigating the relationship between the location of the tremor source in relation to the exploitation front and the tremor energy. The existing experiences and observations indicate that tremor epicentres, and their location in particular, are related to the value of energy emitted during tremor occurrence (Burtan, Zorychta, Chlebowski, & Cieślik, 2016; Kozłowska, 2012, 2013). Statistical analyses show that the greatest number of tremors occur within a distance of less than 50 m from the front line (Kozłowska, 2012, 2013), while the majority of low-energy tremors are located in the area of the face entry drivage, and a considerable number of them take place after blasting and stress relief shooting (Burtan et al., 2016). In turn, the largest number of high energy (especially very strong) tremors occur in the area of opening-up works, whereas a significant part of them are located, ahead of the exploitation front (Burtan et al., 2016).

The vertical location of the foci, which is usually difficult to determine, is closely related to the geological structure of floor formations. Under the conditions of Legnica-Głogów Copper District (LGOM), the layers of anhydrite and dolomitic limestones, as well as local conditions in contact zones between the layers of anhydrite, limestone and dolomite are responsible for the occurrence of high-energy tremors (Zorychta et al., 2005, 2015).

The above observations have become the basis for geomechanical analyses for typical geological and mining conditions occurring in the LGOM. They aimed to determine rock mass areas in the vicinity of the mining exploitation, where significant concentrations of elastic strain energy occur. Geomechanical analyses included FEM numerical calculations and studies of the distribution of the energy density of elastic deformation in the vicinity of the exploitation front performed. The purpose of calculations using the Finite Elements Method (FEM) was to determine the factors and conditions that determine the location of the sources and the mechanism of rock destruction. Appropriate energy measures of elastic deformation energy, in the form of non-shear and volumetric strain energy, were adopted to determine the areas of rock mass potentially threatened with tremors of different energies. These measures allow us to determine the nature of rock mass destruction in the vicinity of mine workings, which in turn gives grounds for linking them with the energy of tremors and their location towards the exploitation front. The results of numerical calculations were compared with the results of statistical analyses, also presented in this paper, concerning the location of tremor sources of different energies in relation to the exploitation front of O/ZG Rudna.

2. Materials and methods

In the geophysical mining station in O/ZG Rudna, the measurements of rock mass seismic activity were realized through the mine seismic system for rock mass observation in a seismic band (up to 150 Hz). Sensors (seismometers) mounted at the deposit level in the chambers in underground mine conditions allow the determination of the rock mass vibration velocity and the transmission of the results of these measurements to the surface, which is carried out by a telecommunication cable network using frequency modulation.

The seismic signal recording process is supervised by dedicated control software, which is responsible for system monitoring, tremor detection, seismic event registration, visualization of seismic channels operation and data transfer to the seismic analyser.

The system of recording vibrations and rock mass seismicity uses 32 seismic channels to locate tremors. They encompass the whole area of the exploited deposit, with several spare stands built in addition to the existing seismic network, which in particular cases (breakdown, need to extend the observation area) can constitute a supplement to the functioning seismological network. These positions combined with surface seismic equipment allow:

- regionalization, loading and notification of seismic event occurrence,
- location of epicentres (sources) of energy tremors exceeding $1.0 \cdot 10^3$ J (with proper visualization on mining maps),
- determination of seismic event energy (based on the integral of the square of ground vibration velocity and the duration of the event),
- evaluation of the character of the event based on the signs of the first waveform input P (longitudinal),
- automatic completion of the database (extract) with parameters characterizing the recorded seismic events.

Results of observation and analysis of the data from the geophysical station in O/ZG Rudna, between 2006 and 2015 (Burtan et al., 2016), enabled the statistical analysis of rock mass seismic activity in O/ZG Rudna and the comparison of its nature and magnitude in subsequent years. The level of this activity was expressed as the number of tremors N for each energy class (A_s>10^3 J) A_s, the aggregate (total) number of the tremors and the aggregate magnitude of the released seismic energy ΣA_s. The formation of seismic activity in the O/ZG Rudna mining area was also considered in terms of mining output, by analysing the following parameters:

- the value of the emitted seismic energy corresponding to the mining output in the whole mine in i-th year A_s^i, J,
- energy expenditure index J^i:

$$J^i = \frac{A_s^i}{W_w^i} \ \text{J/Mg} \tag{1}$$

where:

W_w^i mining output expressed in [Mg] in i-th year.

The Finite Element Method and the Abaqus System (Bathe, 1982; Simulia, 2016; Zienkiewicz & Taylor, 1989, 2000) were used during the geomechanical analyses carried out for typical geological and mining conditions occurring in the LGOM. Numerical calculations using this method can be carried out on different types of rock mass models, two and three dimensional (Pande, Beer, & Williams, 1990; Souley, Hommand, & Thoraval, 1997; Jing, Hannson, Stephansson, & Shen, 1997) assuming physical linear and nonlinear relationship (Cieślik, 2013, p. 286; Jing & Hudson, 2002; Wriggers, 2008) as well as continuity and discontinuity of the medium (Barton, 2013; Cundall, 1988; Wittke, 2014). In this paper, due to the simplified assumption that the projection of the working space and the gobs will be carried out through the rock mass areas of equivalent (post-failure) deformation parameters; the calculations were carried out on a two dimensional (2D) rock mass model. The dimensions of the 2D plane strain model were 370 m × 1000 m. Based on the obtained results, the influence of rock mass structure, roof formations and contact conditions of the individual layers on the distribution of elastic energy density in the vicinity of the exploitation front was analysed. It was assumed that dolomite, dolomitic limestone and anhydrite are deposited in the roof (Fig. 1). For the accepted rock model, the influence of the thickness of the dolomitic limestone layer (considered as potentially tremor-prone) on the distribution of the energy density of elastic deformations was analysed. Two thicknesses of the

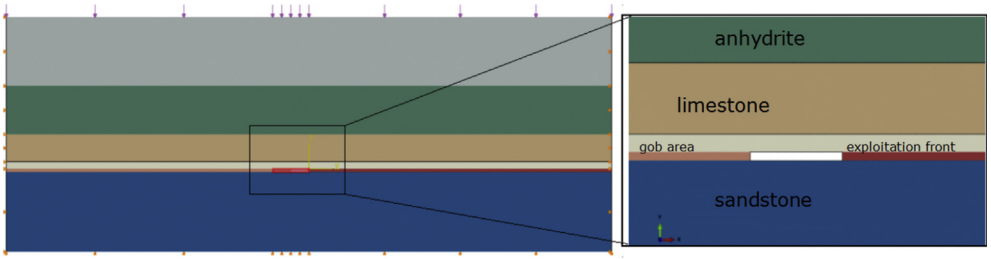

Fig. 1. Geometry of FEM model.

limestone layer were used for the calculations – 40 m and 60 m, as a typical range of limestone layer thickness for O/ZG Rudna geological conditions.

The second factor which, according to observations, has a very significant impact on rock mass seismic activity, was rock mass divisibility defined by the contact conditions between the particular layers. Because of the difficulty in determining the actual conditions of the contact and its parameters, even for the simplest contact models (Barton, 2013; Jing & Hudson, 2002), Coulomb's friction coefficient defined by friction coefficient μ was adopted for calculations. Two extreme values of this coefficient were used for calculations: $\mu = 0$, which corresponded to the free relative displacements of the surfaces of contacting layers and the full tie equated to the lack of possibility of displacements. The contact was defined for layers of dolomitic limestone and anhydrite and the layers surrounding them.

The mining conditions that were taken into account corresponded to the chamber - pillar exploitation system with bending of the roof layer (Zorychta et al., 2005). Geomechanical rock mass properties, mapped by a linear elastic physical model, corresponded to the parameters of mean values of the LGOM rock mass (Table 1).

The displacement of boundary conditions of the models corresponding to zero displacements on the respective vertical and horizontal edges of the model (Fig. 1) were adopted for calculations. The model load was normal vertical stress on the upper horizontal edge of the model and mass forces that represented the rock mass's own weight. The task was solved in several computational steps, which represented the conditions of the initial state of stress in the rock mass and exploitation advance. The problem was treated as geometrically nonlinear, which is why FEM equations in the Abaqus calculation system (Simulia, 2016) were solved using Newton-Raphson's iterative procedure (Simo & Hughes, 1998).

The results of the calculations are presented in the form of maps and graphs of the energy density indexes of deformation energy density:

$$K_{A_C} = \frac{A_c}{A_c^p} \quad K_{A_f} = \frac{A_f}{A_f^p} \quad K_{A_v} = \frac{A_v}{A_v^p} \tag{2}$$

where:

K_{Ac} - total strain energy density index,
K_{Af} - shear strain energy density index,
K_{Av} - volumetric strain energy density index.

Index p was assigned to the values of the individual types of energy corresponding to the initial stress.

Elastic deformation energy density: total A_c, shear A_f and volumetric A_v strain, is defined as follows (Burzyński, 1982):

$$A_c = \frac{1}{2E}\left[\sigma_x^2 + \sigma_y^2 + \sigma_z^2 - 2\nu(\sigma_x\cdot\sigma_y + \sigma_y\cdot\sigma_z + \sigma_z\cdot\sigma_x) + 2(1+\nu)\left(\tau_{xy}^2 + \tau_{yz}^2 + \tau_{zx}^2\right)\right] \tag{3}$$

$$A_f = \frac{1+\nu}{3E}\left[\sigma_x^2 + \sigma_y^2 + \sigma_z^2 - \sigma_x\cdot\sigma_y - \sigma_y\cdot\sigma_z - \sigma_z\cdot\sigma_x + 3\left(\tau_{xy}^2 + \tau_{yx}^2 + \tau_{zx}^2\right)\right] \tag{4}$$

$$A_v = \frac{1-2\nu}{6E}(\sigma_x + \sigma_y + \sigma_x)^2 \tag{5}$$

3. Results

3.1. Characteristics of seismic activity and selected parameters of this activity during exploitation in O/ZG Rudna

A detailed analysis of rock mass seismic activity in the various mining areas of O/ZG Rudna is presented in this paper (Burtan et al., 2016). In this paper, the seismic activity of rock mass is characterized only by the number of recorded phenomena, the total value of energy emissions and the index of unit energy expenditure. The level of activity expressed by the number of tremors N for each energy class (A_s>10^3 J) A_s, the aggregate (total) number of tremors ΣN and the total magnitude of the released seismic energy ΣA_s is shown in Table 2. In turn, the way of forming the total seismic energy value $\log\Sigma A_s$ and total energy expenditure index J for the years of the period considered ΣA_s is illustrated in Figs. 2 and 3.

Table 1
Deformation and strength parameters used in the FEM calculations (Zorychta et al., 2015).

Type of rock	Thickness [m]	Uniaxial Compressive Strength *UCS* [MPa]	Young's Modulus *E* [GPa]	Poisson's Ratio ν [–]
Anhydrite	100	93.1	22	0.24
Dolomite limestone	40–60	117.3	25	0.24
Dolomite	12	140.5	20	0.24
Gangway	4.5	48.2	16	0.25
Sandstone	100	22.8	8.4	0.30
Gobs	4.5	–	0.2	0.45

Table 2
Total number of tremors and the magnitude of released seismic energy.

Year/N/A_s [J]	10^3	10^4	10^5	10^6	10^7	10^8	10^9	ΣN	ΣA_s [J]
2006	1904	467	187	73	19	2	1	2653	$3.28 \cdot 10^9$
2007	1760	543	229	87	21	2	–	2642	$1.22 \cdot 10^9$
2008	1773	700	231	70	12	1	–	2787	$7.65 \cdot 10^8$
2009	1528	598	214	78	33	1	–	2452	$1.36 \cdot 10^9$
2010	1248	510	193	55	27	2	–	2035	$1.16 \cdot 10^9$
2011	1454	629	212	70	23	–	–	2388	$8.18 \cdot 10^8$
2012	1304	678	187	47	20	–	–	2236	$6.95 \cdot 10^8$
2013	1639	730	200	57	10	1	–	2637	$6.51 \cdot 10^8$
2014	1828	739	235	56	6	–	–	2864	$4.45 \cdot 10^8$
2015	1674	722	232	55	3	2	–	2688	$8.47 \cdot 10^8$
(2006–2015)$_{mean}$	**1611**	**631.6**	**212**	**64.8**	**17.4**	**1.1**	**0.1**	**2538.1**	**$1.12 \cdot 10^9$**

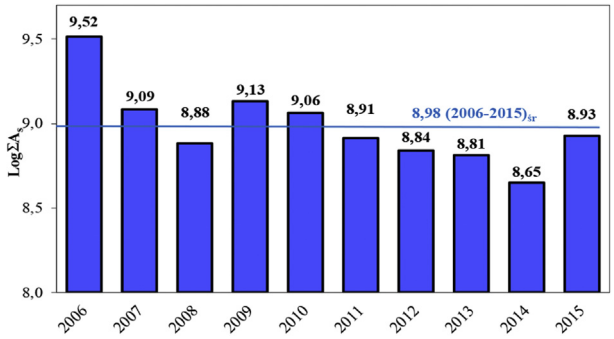

Fig. 2. Distribution of total seismic energy for the years 2006–2015.

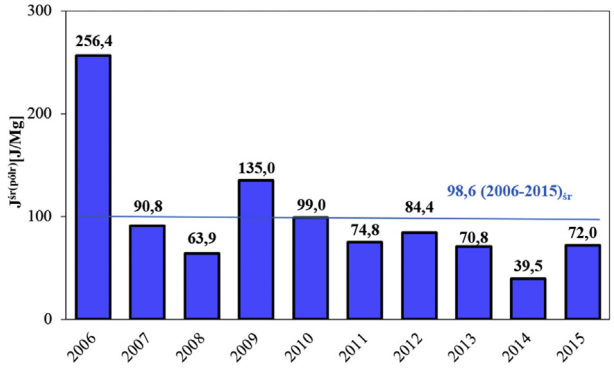

Fig. 3. Distribution of the total energy expenditure index for the years 2006–2015.

The presented data shows that in the Rudna mine during the period from 2006 to 2015, a high comparable level of tremor hazard was present, which was associated with the size of all the analysed parameters of induced seismicity, whereas the above-average values are characteristic for the following years:

- 2014, 2008 and 2015 from the point of view of the total number of registered events (Table 2),
- 2006, 2007 and 2009 and 2010 from the point of view of the total energy emission from the rock mass (Fig. 2),
- 2006 and 2009 from the point of view of energy expenditure index (Fig. 3).

The measurement network of geophysical mining station of the LGOM mines (including also O/ZG Rudna) enables the localization of sources of the recorded tremors not only in the Cartesian spatial coordinate system, but also the verification of their epicentres relative to the location of the exploitation front. It is therefore possible to determine whether a given tremor (its hypocentre or epicentre) has occurred:

- in the unmined coal of the gangway, i.e. ahead of the front of face-entry drivage,
- in the immediate vicinity of the front line of face entry drivage or work area (opening-up of the roof),
- in the gobs – behind the front in the liquidated space.

On the basis of tremor source location data, the seismic activity of the rock mass was analysed in the whole mine, in terms of the number of events and total energy released. The analyses were performed with a distinction between low energy events (in classes 10^3–10^4 J) and high energy events (of the order of 10^5 J and higher).

Figs. 4 and 5 show the percentage share of tremors depending on their location in terms of number of events, and total energy for the entire number of tremors (seismic energies $A_s \geq 10^3$ J), in Figs. 6 and 7 the same dependencies in the energy class 10^3–10^4 J ($10^3 \leq A_s < 10^5$ J), while in Figs. 8 and 9 in the energy class of 10^5 J and higher ($A_s \geq 10^5$ J) (Burtan et al., 2016).

The results of the analyses (Figs. 4–9) clearly indicate that, regardless of the scope (range) of energy and approach variant, the vast majority of sources of the recorded tremors were located in the opening-up zone (at the front), whereas their share has changed by:

- quantitatively: from 52.6% for low energy events (Fig. 6) to 62.4% for high energy events (Fig. 8), with an overall average for the total number of tremors of 53.8% (Fig. 4),
- energetically: from 54.0% for low energy events (Fig. 7) to 72.9% for high energy events (Fig. 9), with an overall average corresponding to the total number of events at 72.4% (Fig. 5).

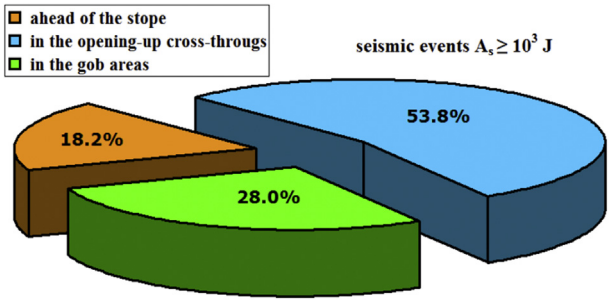

Fig. 4. Percentage share of tremors according to their location in terms of the number of events for the total tremor number.

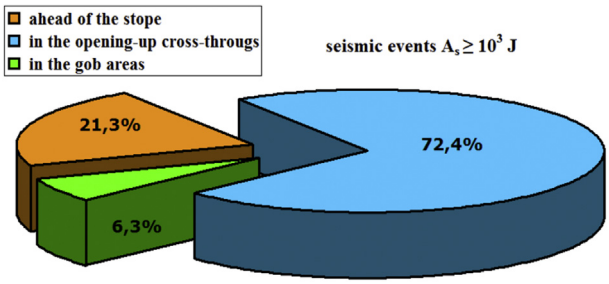

Fig. 5. Percentage share of tremors according to their location in terms of total energy for the total tremor number.

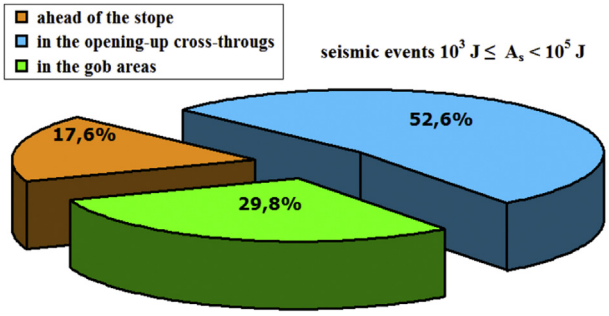

Fig. 6. Percentage share of tremors depending on their location in terms of number of events in the energy class 10^3–10^4 J.

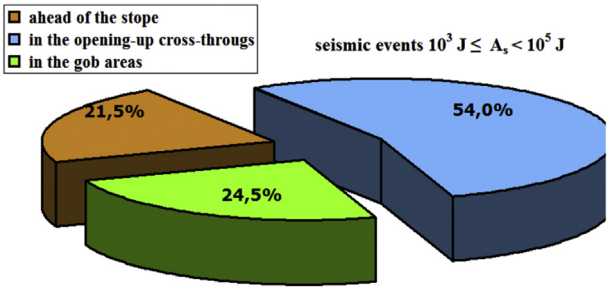

Fig. 7. Percentage share of tremors according to their location in terms of total energy in the energy class 10^3–10^4 J.

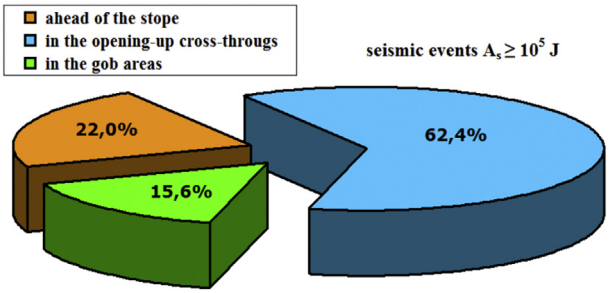

Fig. 8. Percentage share of tremors according to their location in terms of number of events in the energy class 10^5 J and higher.

3.2. Results of FEM Abaqus calculation of the stress state and elastic energy in the rock mass, in the vicinity of the conducted exploitation

In geo-mechanical analyses using FEM, the state of stress was calculated and the density of individual elastic energies

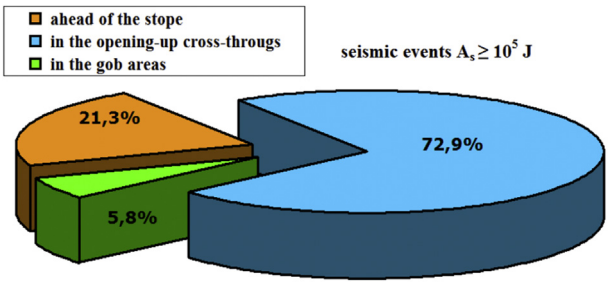

Fig. 9. Percentage share of tremors according to their location in terms of total energy in energy class 10^5 J and higher.

corresponding to them were determined. The purpose of these calculations was to determine rock mass areas in the vicinity of the conducted mining operation, where their significant concentrations occur. As variants of the calculations, a variety of roof structures in the vicinity of the exploitation was assumed (occurrence of the so-called tremor-prone layer of limestone with a thickness of 40 m and 60 m) as was the variable contact conditions of dolomite, dolomitic limestones and anhydrite layers.

The influence of the thickness of the tremor-prone layer on the distributions and values of the individual energy density indices was analysed first. Calculations in this variant were carried out assuming free slip between dolomite, limestone and anhydrite layers, as illustrated in Figs. 10–12.

It follows from the presented maps of the density distributions of elastic energy for both thicknesses of the tremor-prone layers (limestone layers) that the results in both qualitative and quantitative terms are similar. Only in the immediate vicinity of the exploitation front, the maximum values of the individual energy concentration indices for limestone with a thickness of 60 m are higher (Table 3).

The presented distributions of energy density indices show the following regularities:

- The area with the highest K_{Ac} values (Fig. 10a and b) is located in the immediate vicinity of the exploitation front. The thickness of the tremor-prone layer does not have a significant impact on the distribution of this parameter in the vicinity of the exploitation front, yet it has a significant impact on the extreme value for this energy density measure.
- In the case of the concentration ratio of the energy density of shear strain K_{Af}, the areas with maximum values of this occur in the immediate vicinity of the exploitation front (Fig. 11a and b) as well as in the roof and floor of the tremor-prone layer, in close proximity to the exploitation front. There is also some accumulation of this type of energy at the contact point of the gobs and the working space, but it is insignificant compared to the values obtained ahead of the exploitation front. This effect corresponds to the stage of obtaining a specific gob's post failure bearing capacity.
- It is also worth noting the distribution of the energy concentration index of volumetric strain K_{Av}, since concentration areas ($K_{Av} > 1$) are always present ahead of the exploitation front (on the panel length) in the floors of the individual floor layers. From a geomechanical point of view there are also interesting situations where $K_{Av} < 1$, and such regions are present above the working space and in the gobs of the individual floor layers (Fig. 12a and b). This situation, although to a lesser extent, also occurs in the roofs of the individual layers ahead of the exploitation front. This is due to the bending character of the separate floor layers, especially in the free slip variant.

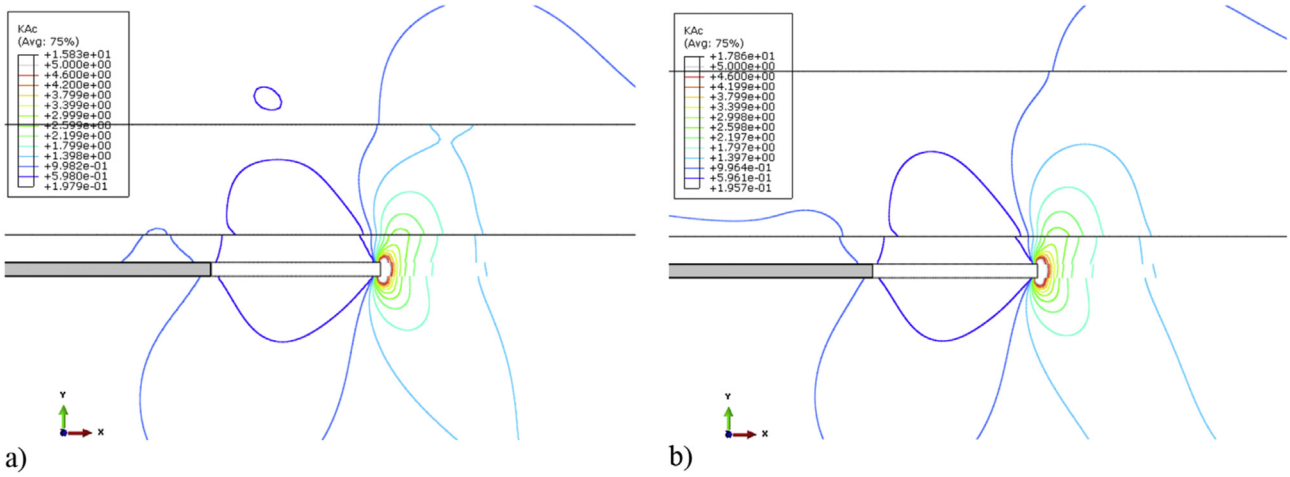

Fig. 10. A map of the energy density index of the total strain.

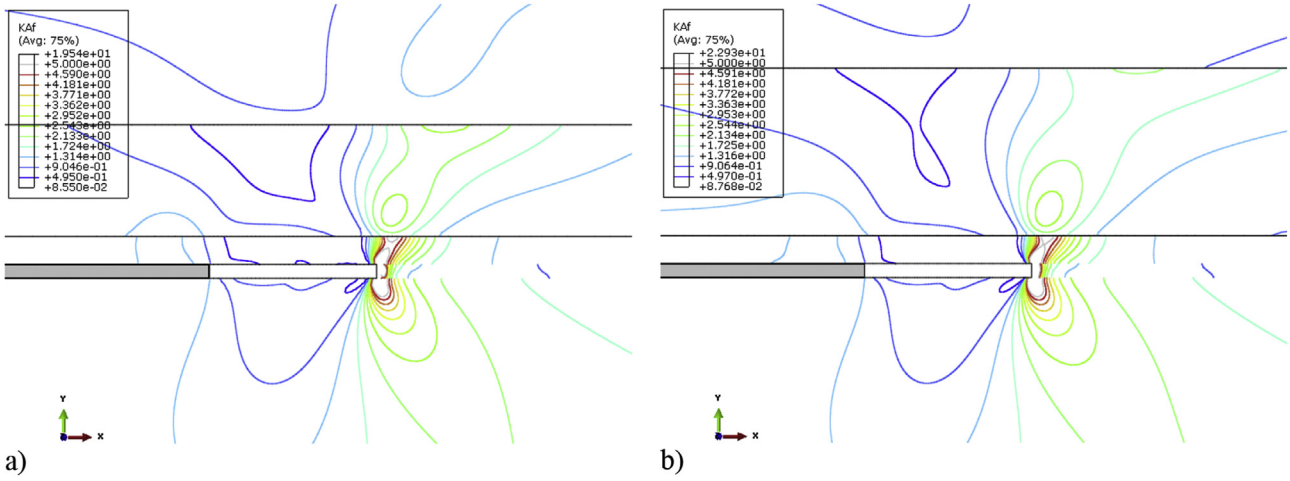

Fig. 11. A map of the energy density index of the shear strain (Burtan et al., 2016).

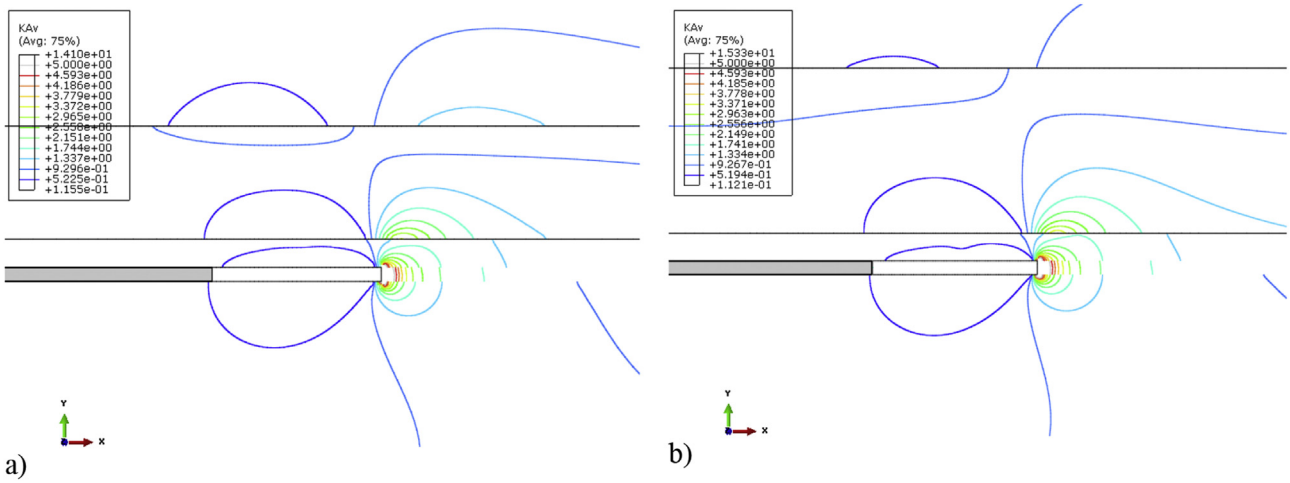

Fig. 12. A map of the energy density index of the volumetric strain (Burtan et al., 2016).

The detailed distribution of the values of individual energy density indices (shear and volumetric strain) in the dolomitic limestone layer (treated as potentially tremor-prone) can be traced in graphs plotted along the line in the roof and floor of this layer (Figs. 13 and 14) for the limestone layer of 60 m.

It should be noted that the extreme values of the individual

Table 3
Maximum values of elastic energy density indices.

Thickness of limestone layer	K_{Ac}	K_{Af}	K_{Av}
40 m	15.8	19.5	14.1
60 m	17.8	22.9	15.3

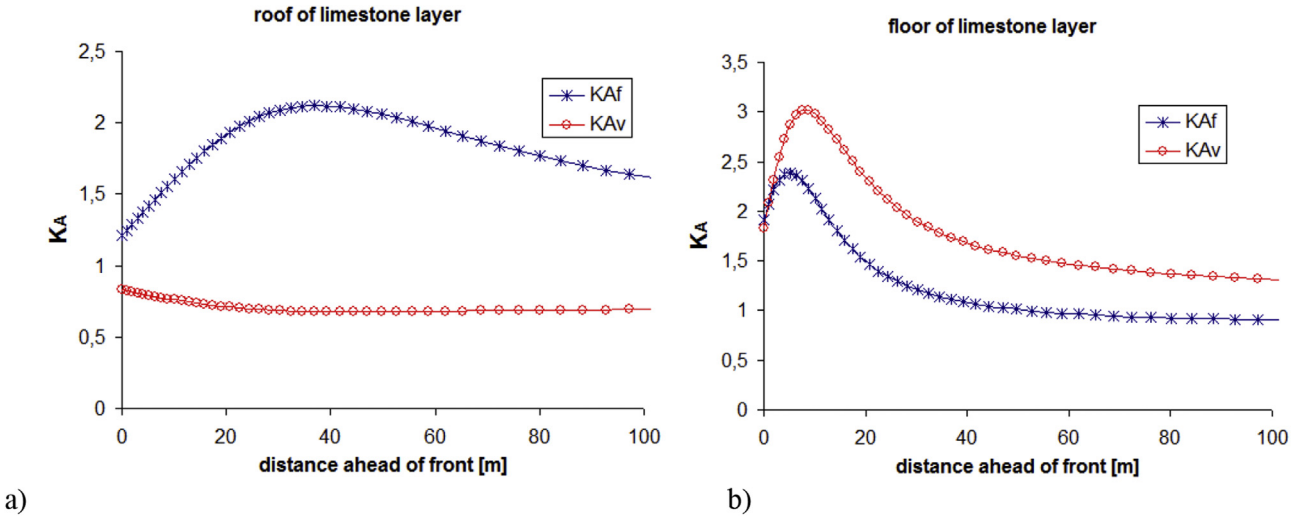

Fig. 13. Graphs of density energy index of shear and volumetric stain in the roof and floor of the limestone layer (60 m thick) in the panel length direction.

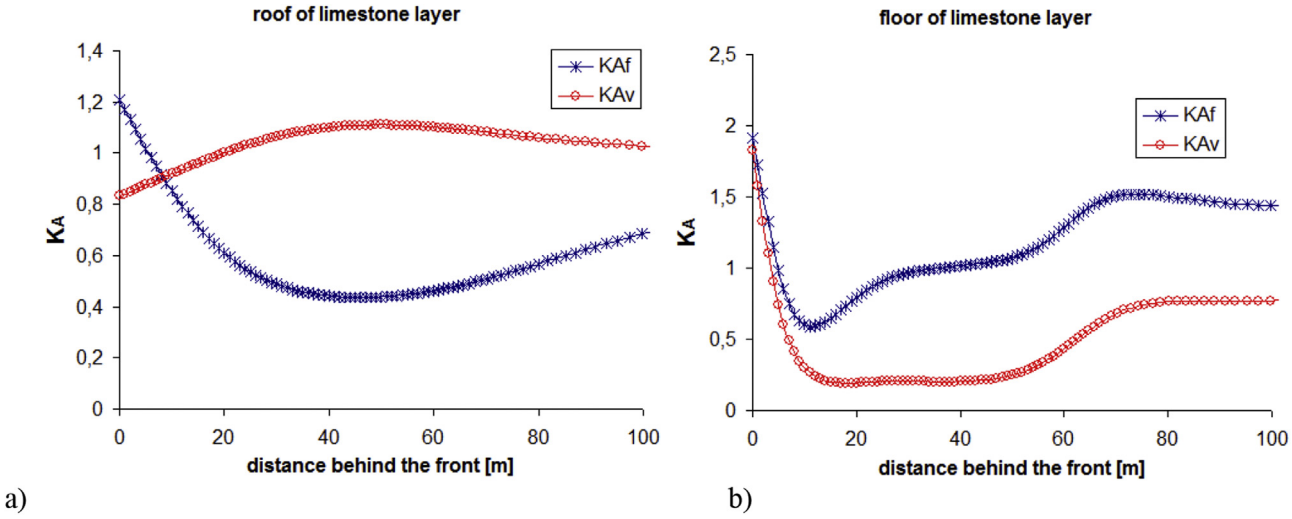

Fig. 14. Graphs of density elastic energy index of shear and volumetric stain in the roof and floor of the limestone layer (thickness 60 m) towards the gobs.

energy concentration indices occur at a distance of no more than 40 m ahead of the exploitation front and 60 m in the direction of gobs. At the panel length, in the roof of the dolomitic limestone layer, there is an increase in the shear strain energy concentration, and the maximum is located at a distance of about 40 m ahead of the front. The extremum energy density of shear stain is accompanied by a gradual decrease in the volumetric strain energy (Fig. 13a). In the limestone roof layer, the volumetric strain energy values as well as values of shear strain initially grow and then decrease to the initial values (Fig. 13b). The extremum of both types of energy falls within the distance of 10 m from the exploitation front.

By analysing the distribution of the various types of elastic energy from the front towards the gobs, it should be stated that their tendencies are reversed in the case of an exploitation front. Over the gobs, in the roof of limestone layers, the energy of the shear strain decreases to a minimum at the distance of approximately 40 m, while the energy of volumetric strain increases (Fig. 14a). Once the maximum is reached, the values of both types of energy rapidly move towards their original values. In the floor, the values of both types of energy abruptly decrease, while the value of the energy index of volumetric strain is at $K_{Av} = 0.25$ and it is significantly lower than the value of the energy concentration ratio of shear strain. At a distance of >60 m (from the front location), the value of both types of elastic energy rises and moves towards its initial value. Qualitative analysis of the distribution of individual

energy concentration indices of elastic energy for a 40 m thick limestone layer is similar to that of a layer with a thickness of 60 m.

The second of the analysed factors influencing the elastic energy distribution within the exploitation front was the contact conditions of the floor layers. According to the assumptions described in Section 2 of this work, two extreme situations were investigated when relative displacement (slipping) between layers of dolomite limestone and anhydrite was free (contact without friction) and slip was not possible (rough contact). The presented results of the calculations (Figs. 15–17) characterize the variant where the thickness of the dolomitic limestone layer was 40 m.

The presented results show the significant influence of contact conditions on the distribution of particular types of elastic energy. In the case when there is a distinct stratified divisibility in the rock mass, which in the computational model corresponded to the free slipping between the dolomite limestone and anhydrite layers, the elastic energy is concentrated in the smaller areas of the rock mass (Figs. 15a, 16a and 17a) than when compared to the absence of this discontinuity (Figs. 15b, 16b and 17b). This phenomenon is particularly visible on maps of the energy density of shear and volumetric strain (Figs. 16a,b and 17a,b).

However, this effect should be referred to as the general rock mass discontinuity, both horizontal and vertical, characterized by various types of discontinuity indices (Jakubowski, 2010, p. 216). In the case of high discontinuity, rock mass has a low tendency to accumulate elastic deformation energy.

4. Discussion

4.1. Characteristics of seismic activity with respect to location relative to the exploitation front

An important feature of the presented quantitative and energetic pie charts (Figs. 4–9) is the variability of the seismic activity in terms of location relative to the exploitation front (large differences in percentages of individual values). At this point it is worth recalling that the rockburst hazard occurring in mine workings increases with the increase in the rock mass tremor energy accompanying mining operation, and the distance of the hypocentre from the working is shorter. In this context, a high share (72.9%) of the energy emitted in the immediate vicinity of the working space (Fig. 9) leads directly to a high level of threat with dynamic events (tremors, stress relief). While for the full hazard assessment it would be necessary to have additional data on spontaneous and provoked events, the observed result may constitute important information for mine services in the context of the direction of the application of appropriate methods and preventive measures, including organizational, technical and active prevention.

Considering the issue in terms of the share of seismic classes (groups), it appears that the lowest number of low-energy tremor sources (in the order of 10^3–10^4 J) is located in the body of coal at the fore-field of the front (17.6% quantitatively, 21.5% energetically Figs. 6 and 7), and high-energy tremors (over 10^5 J) – in the gobs (15.6% quantitatively, 5.8% energetically, Figs. 8 and 9).

Unlike the above, the respective shares for the entire base encompassing all the registered mining tremors of the order 10^3 J upwards. Here, the results of the quantitative analysis illustrate the opposite situation compared to the total energy emitted from the rock mass. They point to the fact that quantitatively the least amount of the analysed tremors was located in the body of the coal (18.2%, Fig. 4), and energetically - in the gobs (mostly its own) behind the exploitation front (6.3%, Fig. 5).

4.2. Geomechanical analysis of the location of tremors sources epicentres

Following Burzyński's material effort definition, according to which brittle material effort (this also refers to rock mass) is determined by the energy of shear strain (Burzyński, 1982) and some part of the volumetric strain energy, it can be assumed that by analysing the concentration regions of the energy density index of shear strain K_{Af}, it is possible to determine areas where effort can be exceeded due to shearing. These zones will therefore be characterized by regions potentially endangered by tremors. Based on the analyses carried out in the previous sections, it can be seen that the concentration of energy density index of shear strain K_{Af}, are present in the areas located ahead of the exploitation front and their maximum values occur within the distance of not more than 40 m from the front (Fig. 13). This is in line with the observations and analyses of epicentre locations of tremor sources, the largest number of which occurs less than 50 m from the front (Burtan et al., 2016; Kozłowska, 2012). The most unfavourable situation from the point of view of high energy tremors occurs when there is a large accumulation of shear strain energy in the region concerned with the simultaneous decrease and a low value (relative to the original)

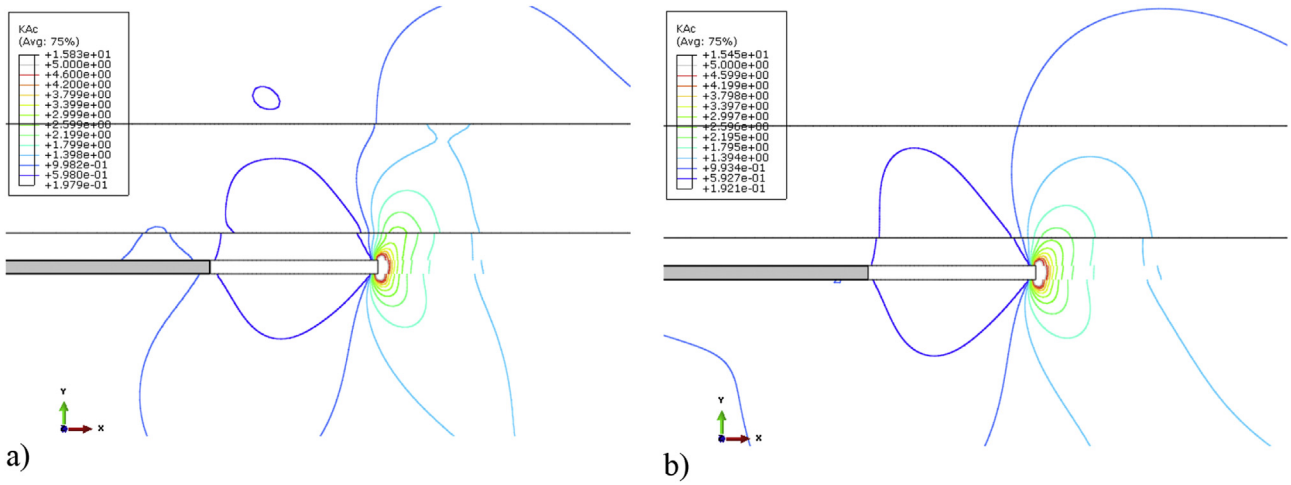

Fig. 15. Map of elastic energy density index of the total strain.

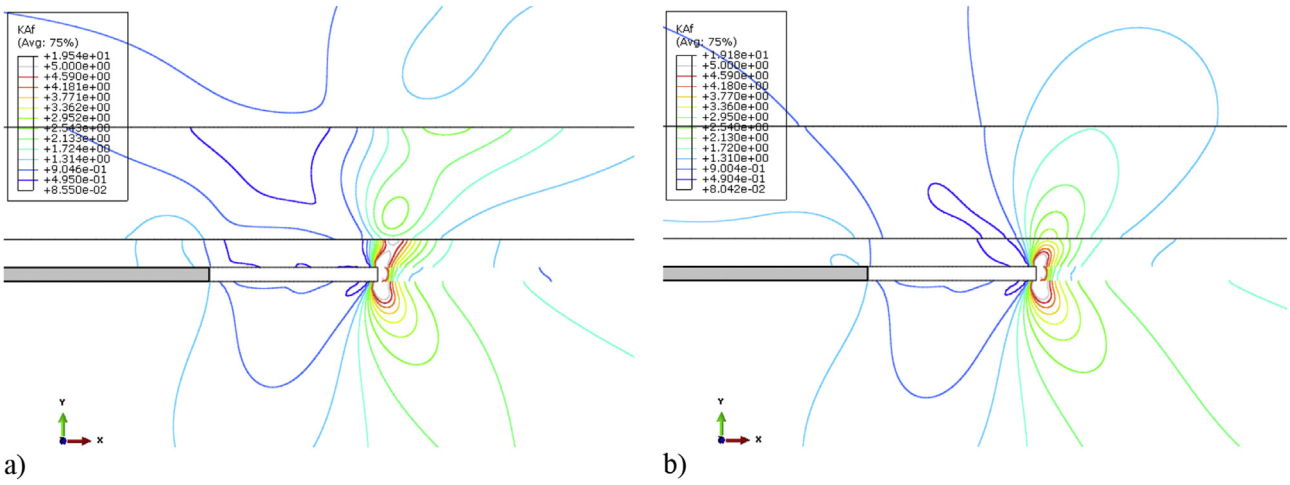

Fig. 16. Map of elastic energy density index of the shear strain.

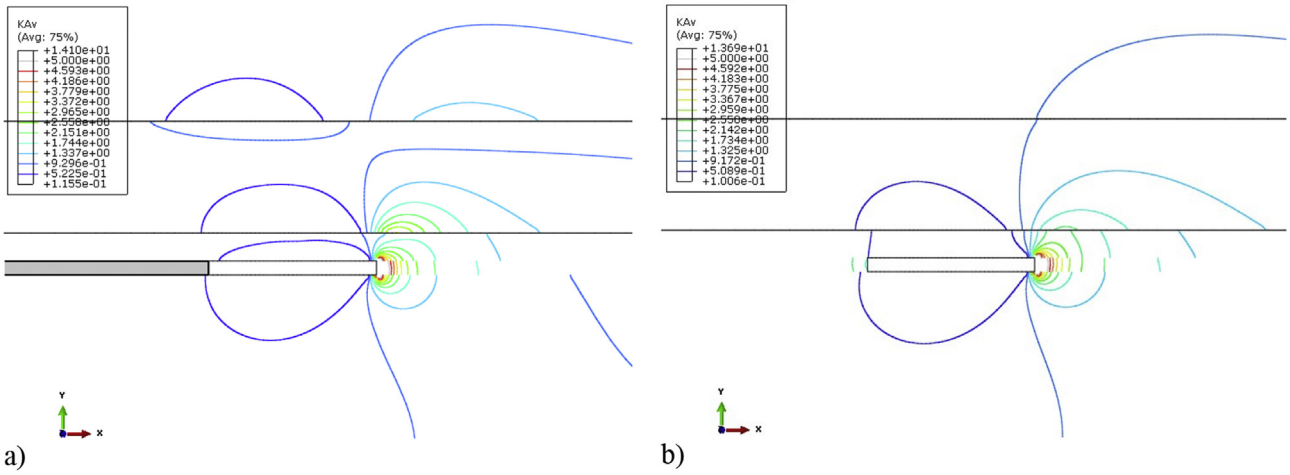

Fig. 17. Map of elastic energy density index of the volumetric strain.

of the energy of volumetric strain. This situation takes place in the floor layers of the tremor-prone layers ahead of the exploitation front (Fig. 13a). At this point, it is also worth noting the possibility of correlating such a mechanism of rock destruction (by shearing) with the geophysical mechanism of the tremor source, in which the shear component plays a dominant role (Gibowicz, Niewiadomski, Wiejacz, & Domański, 1989; Orlecka-Sikora, Papadimitriou, & Kwiatek, 2009; Rudziński & Lizurek, 2015).

The areas where the value of volumetric strain (energy density index of volumetric strain K_{Av}) falls below K_{Av} <1 may be characterized by rock mass areas where potentially low-energy tremors may occur. Based on the analysis of K_{Av} index distribution, it can be assumed that such conditions exist over the gobs or working spaces. At low values of the energy density of non-dilatational and dilatational strain in the roof formations (Fig. 14b), damage can occur by shearing (when K_{Av} <1), or by exceeding the rock mass tensile strength when the K_{Av} value is close to zero. The above observations, resulting from numerical calculations and qualitative geomechanical analyses, are consistent with mine observations and the results of statistical analyses referring to the locations of tremors in relation to the exploitation front (Burtan et al., 2016; Kozłowska, 2012, 2013).

5. Conclusions

On the basis of the rock mass seismicity analysis in O/ZG Rudna for the period 2006–2015, it can be stated that the high level of seismic hazards associated with the number of recorded events, total energy emitted from the rock mass and the value of unit energy expenditure throughout the whole mining area, is comparable to previous years. The annual average value of the emitted energy periodically fluctuated with a general downward trend. It should be emphasized that the data and the results of the analyses have no particular character. This is due to their use for the verification of numerical calculations, that they can therefore be interpreted as typical of the results obtained in the LGOM area.

With regard to the individual energy classes, the number of high-energy tremors (10^5 and 10^6 J) in the period under review is generally at a similar level, and since 2007 there has been a decrease in the number of tremors of 10^8 J. Such a trend occurs in the absence of seismic events of the order 10^9 J. As of 2009, fewer shocks of 10^7 J have been recorded.

On the basis of the conducted analyses a clear relationship is visible between the number of tremors and the size of their energy with source distribution towards the exploitation front. Regardless

of the order of the energy of seismic tremors, the vast majority of phenomena are located at the front of the opening-up works. Taking into account the shares of particular energy classes (ranges), the lowest number of sources in the group of low-energy tremors is located in the body of coal at the fore-front, whereas the group of high-energy tremors are located in the gobs of the exploited fields.

The conducted geomechanical analyses allows the conclusion to be made that the energy of shear strain energy can be treated as a measure of the potential threat of rock tremors. Based on the analysis of the rock mass regions where the highest concentrations take place, it is possible to designate zones in which effort can be exceeded by shearing, resulting in high energy tremors. This situation takes place especially in the case of overlapping zones of high concentration of shear strain energy with zones of low energy of volumetric strain. Such rock mass areas occur in the exploitation panel length. In turn, the elastic energy of volumetric strain, the minimum of which is usually not more than 60 m behind the front, can be a hazard measure of low-energy tremors.

In order to summarise the results of these calculations, which qualitatively match the results of the statistical analysis of the locations of tremors relative to the exploitation front, it should be emphasized that they were obtained on a 2D rock model that corresponds to the in plane bending of the roof over the mine working. In this way the concentration of stresses and the density of elastic energy accumulated in the corners of the exploitation field, in the case when mining is not conducted along the straight line of the front, is neglected. It is in the corners of the exploitation fields that the greatest accumulation of elastic energy can occur, and in these regions, in actual mining conditions, the greatest number of seismic events are to be expected (Zorychta et al., 2015).

On the basis of the performed calculations, it can be further stated that the corresponding geomechanical computer simulations compared with geophysical analysis of tremor mechanism and static stress transfer analysis in the tremor zone (Orlecka-Sikora et al., 2009; Rudziński & Lizurek, 2015; Kwiatek, 2004; Gibowicz et al., 1989) may allow the determination of the regions potentially threatened with tremors (thus the approximate location of tremors sources) and, at least qualitatively, the determination of the level of expected tremor energy.

Acknowledgements

The paper was created within statutory research conducted at the Faculty of Mining and Geoengineering, AGH University of Science and Technology, No. 11.11.100. 277.

References

Barton, N. (2013). Shear strength criteria for rock, rock joints, rockfill and rock masses: Problems and some solutions. *Journal of Rock Mechanics and Geotechnical Engineering, 5*, 249–261.

Bathe, K. J. (1982). *The finite element procedures in engineering analysis*. New York: Prentice Hall.

Burtan, Z. (2011). Kształtowanie się zagrożenia sejsmicznego w trakcie eksploatacji rud miedzi w rejonie strefy uskoku Biedrzychowa [Seismic hazard in the copper mining area adjacent to the fault zone in Biedrzychowa]. *Prace Naukowe Głównego Instytutu Górnictwa. Górnictwo i Środowisko, 4*(2), 34–42.

Burtan, Z., Zorychta, A., Chlebowski, D., & Cieślik, J. (2016). Analiza sejsmiczności indukowanej w O/ZG „Rudna" w aspekcie rozmieszczenia ognisk wstrząsów względem frontu eksploatacyjnego [A geomechanical analysis of high and low-energy tremors, their location and conditions for their occurence during exploitation processes in the LGOM region]. In *Paper presented at XXIII Międzynarodowa Konferencja Naukowo-Techniczna z cyklu Górnicze Zagrożenia Naturalne, Szczyrk, 8–10 listopada 2016*. Katowice: GIG.

Burzyński, W. (1982). *Dzieła wybrane. T. 1*. Selected Works (Vol. 1). Warszawa: PWN.

Chlebowski, D. (2011). Energetyczna ocena możliwości wystąpienia procesów pękania w utworach anhydrytowych na przykładzie oddziału G-22 O/ZG Rudna [Energy-related evaluation of cracking processes occurrence possibility in anhydrite formations on the example of the section G-22 of O/ZG Rudna mine]. *Prace Naukowe Głównego Instytutu Górnictwa. Górnictwo i Środowisko, 4*(2), 43–51.

Cieślik, J. (2013). *Plastyczność i uszkodzenie wybranych skał w testach jednoosiowego i trójosiowego ściskania [Plasticity and damage of selected rocks in uniaxial and triaxial compression tests]*. Kraków: Wydawnictwo AGH.

Cundall, P. A. (1988). Formulation of a three-dimensional distinct element model-Part I: A scheme to detect and represent contacts in a system composed of many polyhedral blocks. *International Journal of Rock Mechanics and Mining Sciences & Geomechanics Abstracts, 25*(3), 107–116.

Gibowicz, S. J., Niewiadomski, J., Wiejacz, P., & Domański, B. (1989). Source study of the Lubin, Poland, mine tremor of 20 June 1987. *Acta Geophysica, 37*(2), 111–132.

Jakubowski, J. (2010). *Stochastyczna symulacja stateczności wyrobisk w nieciągłym masywie skalnym [Stochastic simulation of excavation stability in the discontinuous rock mass]*. Kraków: Wydawnictwa AGH.

Jing, L., Hannson, H., Stephansson, O., & Shen, B. (1997). 3D DEM study of thermo-mechanical responses of nuclear waste repository in fractures rocks – far and near-field problems. In *9th International Conference of the International Association for Computer Methods and Advances in Geomechanics (IACMAG). Wuhan, 2-7 November 1997* (Vol. 2, pp. 1207–1214). Rotterdam: Balkema.

Jing, L., & Hudson, J. A. (2002). Numerical methods in rock mechanics. *International Journal of Rock Mechanics & Mining Sciences, 39*(4), 409–427.

Kozłowska, M. (2012). Ilościowa analiza odległości epicentralnych wstrząsów względem frontu eksploatacji w O/ZG Rudna (LGOM) [Quantitative analysis of epicentral tremors distance in relation to exploitation front in O/ZG Rudna (LGOM)]. *Przegląd Górniczy, 68*(12), 75–85.

Kozłowska, M. (2013). Analysis of spatial distribution of mining tremors occurring in Rudna copper mine (Poland). *Acta Geophysica, 61*(5), 1156–1169.

Kwiatek, G. (2004). Search for sequences of mining-induced seismic events at the Rudna Copper Mine in Poland. *Acta Geophysica, 52*(2), 155–171.

Kłeczek, Z. (2006). Zagrożenie tąpaniami w polskich kopalniach węgla kamiennego i rud miedzi [Risk of rock-mass bursts in Polish Copper Mines (LGOM) and coal mines]. *Bezpieczeństwo Pracy i Ochrona Środowiska w Górnictwie, 6*, 8–12.

Kłeczek, Z. (2007). Sterowanie wstrząsami górotworu LGOM [Control of rock-mass bursts in Polish Copper Mines (LGOM)]. In Z. Pilecki (Ed.), *Materiały sympozjum Warsztaty Górnicze z cyklu "Zagrożenia naturalne w górnictwie" Ślesin, 4–6 czerwca 2007* (pp. 255–261). Kraków: IGSMiE PAN.

Orlecka-Sikora, B., Papadimitriou, E. E., & Kwiatek, G. (2009). A study of the interaction among mining induced seismic events in the Legnica-Glogow Copper District, Poland. *Acta Geophysica, 57*(2), 413–434.

Pande, G. N., Beer, G., & Williams, J. R. (1990). *Numerical methods in rock mechanics*. New York: Wiley.

Rudziński, Ł., & Lizurek, G. (2015). Mechanizm zjawiska sejsmicznego oraz tąpnięcia w O/ZG Rudna w Polkowicach z 19.03.2013 r. z wykorzystaniem lokalnych i regionalnych sieci sejsmologicznych [Source mechanism of 19.03.2013 Rudna's mine, Poland, seismic tremor and following rockburst in a view of local and regional seismic networks]. *Cuprum: Czasopismo Naukowo-techniczne Górnictwa Rud, 3*, 61–72.

Simo, J., & Hughes, T. (1998). *Computational inelasticity*. New York: Springer-Verlag.

Simulia. (2016). *Abaqus v. 6.12 User's manual*. Dassault Systemes.

Souley, M., Hommand, F., & Thoraval, A. (1997). The effect of joint constitutive laws on the modelling of an underground excavation and comparison with in-situ measurements. *International Journal of Rock Mechanics and Mining Sciences & Geomechanics Abstracts, 34*(1), 97–115.

Wittke, W. (2014). Finite element method (FEM). In *Rock Mechanics based on an Anisotropic Jointed rock model (AJRM)* (pp. 8–10). Weinheim, Germany: Wiley-Verlag.

Wriggers, P. (2008). *Nonlinear finite element method*. Berlin: Springer.

Zienkiewicz, O. C., & Taylor, R. L. (1989). *The finite element method. Vol. 1, Basic formulation and linear problems*. London: McGraw-Hill.

Zienkiewicz, O. C., & Taylor, R. L. (2000). *The finite element method. Vol. 2, Solid mechanics*. Oxford: Butterworth-Heinemann.

Zorychta, A., Burtan, Z., & Chlebowski, D. (2005). Wpływ warunków górniczych na kształtowanie się stanu zagrożenia wstrząsami i tąpaniami [An influence of mining conditions on the seismic hazard]. *Cuprum: Czasopismo Naukowo-techniczne Górnictwa Rud, 3*, 33–42.

Zorychta, A., Cieślik, J., Burtan, Z., & Chlebowski, D. (2015). Geomechaniczne warunki poprawy efektywności strzelań torpedujących w kopalniach LGOM [Geomechanical conditions for torpedo blasting efficiency improvement in LGOM mines]. *Cuprum: Czasopismo Naukowo-techniczne Górnictwa Rud, 3*, 83–93.